Biochemical Pharmacology, Vol. 57, pp. 1233–1244, 1999.

ISSN 0006-2952/99/$–see front matter
PII S0006-2952(99)00039-8

An NMR Analysis of the Reaction of Ubiquitin with [*Acetyl*-1-^{13}C]Aspirin

Jeffrey M. Macdonald, Darryl A. LeBlanc,* Arthur L. Haas† and Robert E. London*‡*

*Laboratory of Structural Biology, National Institute of Environmental Health Sciences, Research Triangle Park, NC 27709; and †Department of Biochemistry, Medical College of Wisconsin, Milwaukee, WI 53226, U.S.A.

ABSTRACT. The acetylation of ubiquitin by [*acetyl*-1-^{13}C]aspirin has been studied using 2D NMR methods. Studies performed in a 50:50 H_2O:D_2O medium show doubling of the acetyl carbonyl resonances, indicating that all of the stable adducts formed involved amide linkages. Assignment of the heteronuclear multiple quantum coherence (HMQC) resonances was accomplished based on comparison of resonance intensities with the results of an Edman degradation analysis, pH titration studies of acetylated ubiquitin, and analysis of two ubiquitin mutants, K33R and K63R. The presence of a single tyrosine residue in close proximity to lysine-48 suggested another assignment strategy. Nitration of tyrosine-59 resulted in a small, pH-dependent shift of the resonance assigned to lysine-48, with a pK of 7.0, close to that expected for the nitrotyrosyl hydroxyl group. An additional adduct resonance with very low intensity also was observed and tentatively assigned to the acetylated N-terminal methionine residue. The relative rates of acetylation of the various lysine residues were obtained from time-dependent HMQC studies. Since no sample preparation artifacts were introduced, the levels of modification of the various residues could be determined with relatively high accuracy. Based on the time-dependent intensity data, the relative rate constants for modification of K6, K48, K63, K11, K33, and M1 were 1.0, 0.59, 0.43, 0.26, 0.23, and 0.03, respectively. These results were in much better agreement with amino accessibility predictions based on the crystal structure of the ubiquitin monomer than with predictions based on the ubiquitin structure in the crystallized dimeric and tetrameric forms. This approach provides a useful basis for understanding how local environmental factors can influence protein adduct formation, as well as for comparing the extent and specificity of various acetylation reagents. BIOCHEM PHARMACOL **57**;11:1233–1244, 1999. © 1999 Elsevier Science Inc.

KEY WORDS. NMR; aspirin; ubiquitin; protein adducts; protein modification; acetylation; histidine acetylation

Although prostaglandin synthase is thought to be the primary physiological target of acetylation by aspirin [1–3], many other targets exist, including serum albumin [4, 5] and hemoglobin [6, 7]. Indeed, acetylation of proteins other than prostaglandin synthase is probably important both in explaining the broad range of physiological effects of this drug and in understanding some of the toxic side-effects. For example, acetylation of hemoglobin by aspirin affects the binding of the physiological effector diphosphoglycerate, altering oxygen affinity as well as the tendency of hemoglobin S to sickle [6–8]. To understand better the chemical basis for such effects, it is necessary to understand how the structural environment of the target residues affects the chemistry of transacetylation. Although NMR has often been used to characterize protein adducts, there have been surprisingly few applications of modern 2D NMR methods to the characterization of adduct formation [9–13]. Hence, an additional goal of the present studies was the more general development of NMR as a tool for the analysis of protein adducts. Further, although isotopic labels can be introduced in either the adduct or the protein, isotopic labeling was limited to the organic reactant, to develop a more general and considerably less expensive approach.

We have selected the protein ubiquitin as a model system on which to study this surface chemistry. Ubiquitin is an unusually stable, highly conserved protein of 76 amino acids lacking an active site, and there is a large body of literature related to the NMR characterization of the protein [14, 15], making it an attractive model system for study. Through a complex series of ATP-dependent reactions, multi-ubiquitin chains are assembled on the substrate proteins and target the substrates for degradation by the 26S proteasome. Recently, additional roles for ubiquitination in cell surface receptor targeting and protein kinase-dependent signaling pathways have been discovered (recent reviews include Hochstrasser [16], Johnson and

‡ Corresponding author: Dr. Robert E. London, Laboratory of Structural Biology, MR-01, National Institute of Environmental Health Sciences, Box 12233, Research Triangle Park, NC 27709. Tel. (919) 541-4879; FAX (919) 541-5707; E-mail: london@niehs.nih.gov

Received 2 July 1998; accepted 16 October 1998.

Hochstrasser [17], and Varshavsky [18]). Two groups of researchers have previously studied the acetylation of ubiquitin using the reagent *p*-nitrophenylacetate. Jabusch and Deutsch [19] found the order of acetylation to be Lys-6 > Lys-11 ~ Lys-33 ~ Lys-48 ~ Lys-63, with Lys-27 and Lys-29 showing little reactivity, and also reported no acetylation of the N-terminal α-amino group. Zhu *et al.* [20] reported similar results, although in both cases, information about the lysine residues furthest from the N-terminal is incomplete and inconclusive. The somewhat qualitative nature of these conclusions relates to the limitations of using the Edman degradation for too many cycles. Mass spectrometry provides a useful method for the characterization of protein modification [21, 22]; however, the analysis is hampered by the high resistance of ubiquitin to proteolysis by trypsin and other proteases. Mass spectrometric analyses also are limited by the need to obtain fragments with single lysine residues, and in the case of trypsin analysis, by limitations on the detection of low molecular weight fragments arising from tryptic digests corresponding to closely spaced lysine residues. To obtain data for single lysine residues, sequential HPLC separation sometimes is necessary, leading to potential errors due to sample handling [22]. Determination of rates of modification of individual residues requires extensive sample handling [21] and is performed infrequently. Jabusch and Deutsch [19] also studied the degree of lysine acetylation to explore the possibility that the anti-inflammatory effects of aspirin might result from acetylation of ubiquitin, resulting in an inhibition of its function in ATP-dependent proteolysis. However, the relatively low rates of lysine acetylation at physiological concentrations tended to rule out this possibility. The present study reports the first 2D NMR analysis of protein acetylation by aspirin and the first study of the kinetics of protein modification in real time.

MATERIALS AND METHODS

Materials

Ubiquitin, tetranitromethane, *N*α-acetylmethionine, *N*α-acetyllysine, *N*α-acetyltyrosine, *N*,*O*-diacetyltyrosine methyl ester, *N*α-acetylserine, *N*α-acetylserine, *N*α-acetylcysteine, *N*-acetylimidazole, and *N*α-acetylhistidine were obtained from the Sigma Chemical Co. Methylene chloride, iodomethane, pyridine, deuterium oxide, deuterium chloride, and deuterium hydroxide were purchased from the Aldrich Chemical Co. Potassium phosphate dibasic and monobasic salts were purchased from Mallinckrodt. Two types of dialysis membrane were used: 2-kDa molecular mass cutoff Slide-A-Lyzer™ cassettes and 3-kDa molecular mass cutoff Spectra/Por® membranes were purchased from Pierce and Spectrum Medical Industries, Inc., respectively. Salicylic acid was purchased from Fluka. Ethanol was purchased from Pharmacia. [1-^{13}C]Acetyl chloride was purchased from Isotec, Inc. The PTH* amino acid standards, including α-PTH-*N*ε-phenylthiocarbamyl lysine (PTH-ε-PTC lysine), were purchased from Perkin-Elmer-Applied Biosystems. PTH-*N*ε-acetyllysine, used as a standard for the Edman degradation study, was purchased from SynPep.

Synthesis of [1-^{13}C]Acetylsalicylic Acid

[1-^{13}C]Acetylsalicylic acid or [2-^{13}C]acetylsalicylic acid were synthesized following an approach similar to that described by Gerig *et al.* [23] by the reaction of [1- or 2-^{13}C]acetyl chloride with salicylic acid. Salicylic acid (1.5 g) was dissolved in 90 mL methylene chloride containing 1.8 mL pyridine. A solution of 20% [1-^{13}C]acetyl chloride in methylene chloride (14 mL) was added. The reaction container was capped and allowed to react for 15 hr at 22°. The reaction container was uncapped, the methylene chloride was evaporated by heating (*ca.* 45°), and then the sample was lyophilized. The purity of the [1-^{13}C]acetylsalicylic acid was determined by ^{1}H NMR to be > 99%. The isotopically labeled aspirin was stored in a desiccator at 0°.

Preparation of Nitrated and [1-^{13}C]Acetyl Stock Ubiquitin

All ubiquitin was dialyzed two times against 4 L of water to remove excess glycine, which is a significant contaminant of the commercial material. Stock [1-^{13}C]acetylubiquitin was prepared by dissolving dialyzed ubiquitin in 1.4 mL of 0.3 M phosphate buffer (pH 7.0) containing 120 mM [*acetyl*-1-^{13}C]salicylic acid, resulting in a molar ratio of 15:1 for [1-^{13}C]acetylsalicylate to ubiquitin. After 24 hr at 37°, the reaction mixture was dialyzed two times against 4 L of water and then lyophilized. Stock [*acetyl*-1-^{13}C]ubiquitin was stored in a desiccator at 4°.

Nitrated ubiquitin was prepared using a procedure essentially as described by Riordan and coworkers [24]. Briefly, tetranitromethane was added to stock [*acetyl*-1-^{13}C]ubiquitin at a molar ratio of 100:1. The tetranitromethane (69 μL) was dissolved in 150 μL of ethanol, and the solution was added to the stock [1-^{13}C]acetylubiquitin dissolved in 0.5 M phosphate buffer (pH 8.1) and allowed to react for 20 hr at 20°. The reaction mixture was lyophilized and then dialyzed extensively against water.

NMR Studies

All NMR studies were performed on a Varian UNITY *Plus* 500 MHz NMR spectrometer, except for the amino acid/aspirin kinetic studies, which were performed on a UNITY *Plus* wide-bore 400 or UNITY 500 MHz NMR spectrome-

* *Abbreviations*: PTH, α-phenylthiohydantoin; PTH-*N*ε-acetyllysine, cyclic-*N*α-phenylthiohydantoin-*N*ε-acetyllysine; PTC, phenylthiocarbamyl; [1′-^{13}C]aspirin = [*acetyl*-1-^{13}C]aspirin = [1-^{13}C]acetylsalicylic acid; HMQC, heteronuclear multiple quantum coherence; TSP, 3-(trimethylsilyl)-propionic-2,2,3,3-d_4 acid; and BIRD, bilinear rotation decoupling.

ter. HMQC spectra were obtained using a 5-mm Nalorac triple resonance probe. Typical HMQC spectral parameters were: spectral width of 4504.5 Hz and 2048 complex data points yielding an acquisition time of 0.455 sec with ^{13}C WALTZ16 decoupling during acquisition, interpulse delay of 0.4 sec, scalar evolution delay of 61 msec, and 0.4 sec presaturation pulse. Typically, the t1 dimension had a spectral width of 628.6 Hz and 64 increments and was collected in phase-sensitive mode. The number of increments and/or transients was varied to obtain the required resolution or signal-to-noise ratio. Two-dimensional spectra were zero-filled to 4096 in t1, and apodization consisted of a shifted sine-bell function. Peak volumes were calculated using the Varian VNMR software (version 5.3b) and referenced to aspirin at 174.2 ppm (^{13}C) and 2.34 ppm (^{1}H) when visible in the 2D spectrum. To assess the effects of the relatively short (0.9 sec) recycle time, spectra were obtained on a highly acetylated ubiquitin sample using an interpulse delay of 11 sec. Saturation factors for each adduct resonance were calculated as the ratio of peak volumes obtained from the overpulsed spectra to those in the fully relaxed (11 sec delay) spectra. For the three most highly modified resonances (corresponding to residues K6, K48, and K63), the saturation factors were in close agreement: SF = 0.643 ± 0.01. If the weaker adduct resonances were also used, the mean value was lower and showed greater variation: SF = 0.59 ± 0.025. This result may indicate a greater saturation effect (longer T_1 values) for the weaker adduct resonances, which are assigned to adducts formed with residues K11, K33, and M1. However, since the error involved in quantitation of the smaller resonances is also larger, we have ignored these differences.

AMINO ACID CHEMICAL SHIFT ASSIGNMENTS. The shift assignments of the *O*-acetyl esters of tyrosine and serine were derived from spectra of commercial *O*-acetyl-L-serine, *N*α-acetyltyrosine, and *N*,*O*-diacetyltyrosine methyl ester. The ^{1}H and ^{13}C chemical shifts of the acetyl groups in *N*- and *S*-acetylated amino acids were determined by reacting *N*α-acetyl amino acids with either [1′ or 2′-^{13}C]aspirin. For *N*α-acetylhistidine, three time-course experiments were performed using direct ^{1}H and ^{13}C observation, and subsequently the first slice of the HMQC experiment to correlate ^{1}H and ^{13}C chemical shifts. Once the ^{13}C chemical shifts were assigned, a ^{13}C spectrum was obtained with high digital resolution, so that accurate ^{13}C chemical shifts could be measured. The two-bond carbonyl ^{13}C methyl–^{1}H coupling constant values ($^{2}J_{CH}$) were measured in the ^{1}H spectrum of *S*- and *N*-acetylated amino acids reacted with [1′-^{13}C]aspirin.

Typically, amino acids were dissolved in 0.15 to 0.25 M phosphate buffer in 100% D_2O (pH 7.0) at various concentrations at 37°. For lysine, histidine, and cysteine, [*acetyl*-1-^{13}C]salicylic acid was added to the mixture at 40–80 mM and allowed to react for 24 hr. Resonances were identified in the ^{1}H and ^{13}C 1D spectra of [*acetyl*-1-^{13}C]amino acid derivatives by the ^{13}C-^{1}H (i.e. J_{CH}) and ^{13}C-^{13}C (i.e. J_{CC}) coupling constants, respectively. For the unlabeled *O*-acetyl esters of serine and tyrosine, the ^{1}H methyl resonance was identified by chemical shift or comparison to the ^{1}H spectra of the corresponding *N*-acetyl amino acids. The ^{13}C methyl and carbonyl resonances were identified from HMQC and heteronuclear multiple bond correlation spectra, respectively, by correlation to the known ^{1}H methyl resonance. The ^{1}H spectra were obtained using a one-pulse sequence, and the ^{13}C spectra were obtained using a one-pulse sequence with ^{1}H decoupling during acquisition using WALTZ16. For acetylated derivatives of serine, tyrosine, and imidazole, the ^{1}H spectra were obtained using a one-pulse sequence with presaturation pulse of 1.5 sec. The ^{13}C spectra were obtained with a 30° flip angle using a one-pulse sequence with GARP-1 ^{1}H decoupling. The ^{1}H and ^{13}C spectra were zero-filled to 65,536 or 131,072 total data points before Fourier transformation, resulting in digital resolution ranging from 0.37 to 0.18 ppb in the proton domain and 7.4 to 3.7 ppb in the ^{13}C domain. The HMQC spectra were obtained with sweep widths in t1 and t2 of 25,156.4 Hz and 6024.1 Hz, respectively, 2048 total data points, scalar evolution delay of 7.14 msec (i.e. **J = 140** Hz), presaturation pulse of 1.5 sec, and 512 increments in t1. The heteronuclear multiple bond correlation spectra were obtained under conditions similar to those for the HMQC spectra, except that the scalar evolution delay was 55 msec and the presaturation delay was 1 sec. The NMR parameters for the time-course studies with histidine are given below. The ^{13}C and ^{1}H chemical shifts were referenced to TSP at -2.0 and 0 ppm, respectively.

KINETIC STUDIES. The kinetics of the histidine acetylation by aspirin were determined by reacting 64 mM *N*-acetyl-α-histidine with 40 mM [*acetyl*-2-^{13}C]salicylic acid in 200 mM phosphate buffer (pH = 7.02) in 100% D_2O at 37°. The first slice of the HMQC was obtained using a sweep width of 4504.5 Hz, 9024 complex data points, resulting in an acquisition time of 1 sec. The interpulse delay was 19 sec, a scalar evolution delay of 61 msec, and each spectrum was composed of 80 transients resulting in a 27-min temporal resolution.

The kinetics of aspirin acetylation of ubiquitin were studied using a solution containing 8.3 mM ubiquitin and 40 mM [*acetyl*-1-^{13}C]salicylic acid in 0.2 M phosphate buffer (pH 7.4) and 100% D_2O. In addition to the HMQC parameters as described above, an inverse BIRD pulse was placed in front of the HMQC sequence to suppress the increasing acetate signal, which co-resonates with the signals of interest. The inverse BIRD sequence is essentially a spin echo with scalar evolution delay of 78.1 msec, a presaturation pulse of 0.4 sec, and a 1.063-sec delay before the start of the HMQC sequence. Each spectrum was composed of 32 transients resulting in a temporal resolution of 3 hr. To determine whether the relative reactivities of the various ubiquitin residues with aspirin were affected by potential protein aggregation, we also treated 0.5 and 2.1

mM ubiquitin solutions as described above. The buffered ubiquitin/aspirin solutions were maintained at 37° for 20 hr, after which they were dialyzed against 3 L of water and lyophilized. The ^{1}H-{^{13}C}-HMQC pulse sequence without the inverse BIRD using the parameters described above was used to obtain 2D spectra. The peak volume ratios of the various adduct resonances were compared with those using 8.3 mM ubiquitin in the reaction mixture. Over this 16.6-fold concentration range, the relative degree of modification of the various resonances varied by less than 20%, and in most cases by smaller factors. Hence, subject to the above error, there was no significant effect of aggregation upon the relative levels of modification among the different ubiquitin residues.

DEUTERIUM-ISOTOPE EFFECT. The deuterium isotope effect [25] was demonstrated using a ubiquitin sample that had been reacted with [1-^{13}C]acetylsalicylic acid for 24 hr in 0.2 M phosphate buffer (pH 7.4) in 100% D_2O. An HMQC spectrum was obtained initially on the sample in 0.2 M phosphate buffer (pH 7.0). Then the sample was lyophilized and re-dissolved in 50:50 D_2O:H_2O (pH 7.42), and an HMQC spectrum was obtained using the same parameters.

PH TITRATION STUDIES. The titration curves of the various resonances in the 2D NMR spectra of nitrated and stock ubiquitin were obtained in 40 mM phosphate buffer, in 100% D_2O and titrated with DCl or NaOD. The 2D HMQC NMR spectra were obtained using the same NMR parameters as described above. The spectra were referenced to the residual aspirin acetyl ^{1}H methyl and ^{13}C carbonyl resonances at 2.34 ppm and 174.2 ppm, respectively. pH titration data were fit to the function

$$\delta_{obs} = \frac{\delta_H + \delta_L 10^{pK-pH}}{1 + 10^{pK-pH}} \quad (1)$$

which assumes simple Henderson–Hasselbalch relationship of shifts to pH described by a single pK value, with δ_H and δ_L the limiting chemical shifts at high and low pH, respectively.

Protein Sequencing

Stock [1-^{13}C]acetylubiquitin was sequenced with an Applied Biosystems 477A protein sequencer at the University of North Carolina Protein Chemistry Laboratory. Edman degradation products were separated on an Applied Biosystems C18 HPLC column (250 mm × 4.6 mm i.d.) using a non-linear gradient composed of buffer A [94.7:3.5:1.8 H_2O:THF:premix buffer (Applied Biosystems)] and buffer B (90:10, acetonitrile:isopropanol) at a flow rate of 210 μL/min and total run time of 31 min. All amino acids and acetylated lysine were baseline-resolved and detected spectrophotometrically by absorbance at 270 nm. The concentrations of PTH-*N*ε-acetyllysine and PTH-ε-PTC lysine resulting from the 70 chromatograms were plotted using the software Mathematica (Wolfram Research).

Ubiquitin Mutants

K33R and K64R mutants were prepared as described by Baboshina and Haas [26]. Mutant ubiquitin (0.4 mM) and [1-^{13}C]acetylsalicylic acid (20 mM) were reacted in 150 mM phosphate buffer in D_2O at 37° for 24 hr. The acetylated mutants were dialyzed two times against 4 L of water to remove excess aspirin and acetate. HMQC spectra were obtained before and after dialysis.

Calculations of Surface Accessibility

Surface accessibilities of the ε-amino groups of lysine residues and the Met-1 α-amino group were determined from the crystal structure [27] using the Connolly algorithm with variable probe radii within the software INSIGHT II (Release 95). This approach provides a contact area and a re-entrant area for each residue. In general, there was an inverse correlation between the calculated contact area and the re-entrant area, so that the total accessible areas calculated according to this method tended to be less variable than the contact areas. Inclusion of the three amino protons with the nitrogen leads to an inherently bumpier surface, so that in all cases, the contact areas become smaller and the re-entrant areas larger. Since inclusion of the protons led to only limited and fairly predictable quantitative changes, we have reported the contact areas of the bare amino groups. This has the additional advantage of avoiding steric problems, which can arise when protons are introduced into the crystal structure. Some calculations were also performed utilizing energy-minimized structures; however, the results strongly depended on details of the minimization process, and occasionally gave unexpected variations due to folding of the lysine side chains nearer to the protein surface. Hence, the most useful evaluations were found to be derived from determination of the contact areas of the bare amino groups using the crystal structure without further alterations.

RESULTS

Chemical Shifts of Acetylated Amino Acid Residues

Since aspirin is in principle capable of acetylating many different functional groups, the shifts of various acetylated amino acids were determined under standard conditions, and are summarized in Table 1. In general, only the acetylcysteine residue gives sufficiently unique chemical shifts to be readily identified on the basis of shift behavior alone. However, ubiquitin is devoid of cysteines. *In vitro* studies of the acetylation of *N*-acetylhistidine by aspirin, presented below, indicated that the acetylated imidazole moiety is fairly unstable. This is not surprising, since acetylimidazole is itself an acetylating agent. In general, it is expected that several species of acetylimidazole should

TABLE 1. NMR data for acetylated amino acids

Compound	Methyl shifts		Carbonyl shifts	$^2J_{CH}$ (Hz)
	^1H	^{13}C		
Acetate	1.92	24.13	182.14	6.1
Aspirin	2.34	21.44	174.2	7.0
N-Acetyllysine*	1.98	22.4	174.47	6.2
N-Acetylhistidine*	2.12	22.95; 22.91	173.29; 173.23	—
N-Acetylimidazole*	2.12	22.9; 22.88	173.25; 173.19	—
O-Acetylserine	2.14	20.94	174.44	—
O-Acetyltyrosine	2.34	21.27	174.36	—
S-Acetylcysteine*	2.39	24.1	201.30	6.2

Samples were prepared in 90% D_2O, 37°C, pD 7.0 (uncorrected meter reading), at concentrations ranging between 0.5 and 50 mM. ^{13}C and ^1H spectra were referenced to TSP at −2.0 and 0 ppm, respectively. All spectra were obtained on a UNITY Plus 400 MHz or UNITY 500 MHz NMR spectrometers.

*Acetylated with [1′-^{13}C]-aspirin. Methyl and carbonyl shifts refer to the acetylated side chain.

form: *N*τ-acetyl, *N*π-acetyl, and *N*τ,*N*π-diacetyl. However, the *N*τ,*N*π-diacetyl derivative of histidine has been reported to be unstable, breaking down to give a diacetamide derivative with an opened imidazole ring and loss of the C_2 ring carbon [28]. In the present studies, spectra of commercial *N*-acetylimidazole and of histidine acetylated with the labeled aspirin revealed pairs of ^1H and ^{13}C resonances in a 54:46 ratio, arising from the *cis-trans* isomerism of imide bond:

In the ^{13}C spectra, the methyl and carbonyl resonances exhibited shift differences of 0.038 and 0.066 ppm, respectively. No further multiplicity arising from differences in the shifts of *N*π- and *N*τ-acetylated histidine and no evidence of *N*π,*N*τ-diacetylated histidine were detected.

Acetylation Kinetics

Since the formation of acetylimidazole from the reaction of aspirin with histidine residues can be transient, time-dependent acetylation studies were performed on a buffered solution containing initially only *N*α-acetylhistidine and aspirin. The time-dependent intensities of the acetyl carbon resonances corresponding to aspirin and acetate and to the acetylimidazole resonances of acetylated histidine are shown in Fig. 1. Neglecting differences in the acetylation rates for Nτ and Nϵ, the acetylation kinetics are described by the relations:

$$\text{Asa} \xrightarrow{k_1} \text{Sal} + \text{Ace}$$

$$\text{Asa} + \text{His} \xrightarrow{k_2} \text{AcHis}$$

$$\text{AcHis} \xrightarrow{k_3} \text{Ace} + \text{His}$$

where Asa = acetylsalicylic acid (aspirin), Sal = salicylate, Ace = acetate, His = *N*α-acetylhistidine, and AcHis = *N*α,*N*τ-diacetylhistidine + *N*α,*N*π-diacetylhistidine + 2*N*α,*N*τ,*N*π-triacetylhistidine. Of course, the *N*α-acetyl group is present to block acetylation of the α-amino group and does not get labeled, and does not contribute to the AcHis intensity. The corresponding fluxes are described by:

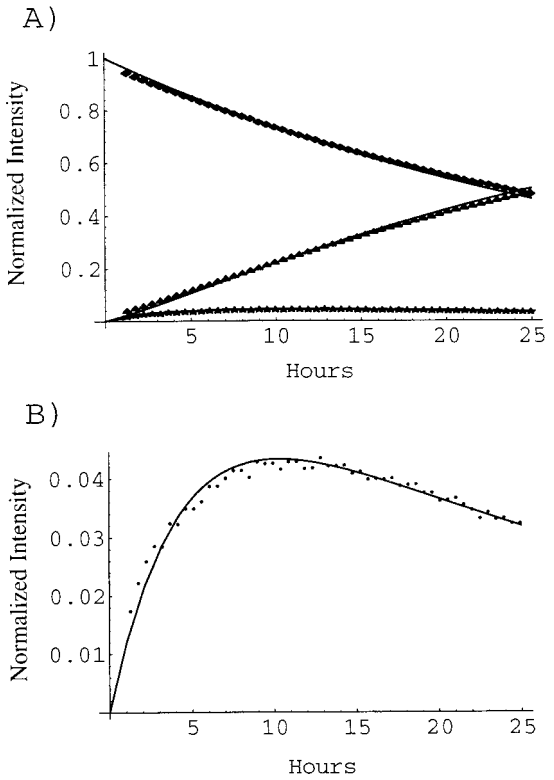

FIG. 1. (A) Intensities of the aspirin (♦), acetate (▲), and acetylhistidine (⋆) resonances as a function of time. Sample initially contained 38 mM [*acetyl-2-*^{13}C]aspirin, 61 mM histidine in 100% D_2O and 212 mM phosphate buffer, pH 7.0 and 37°. (B) Expansion showing the acetylhistidine intensities.

$$\frac{dAsa(t)}{dt} = -k_1 Asa(t) - k_2 Asa(t)\,His(t)$$

$$\frac{dHis(t)}{dt} = -k_2 Asa(t)\,His(t) + k_3 AcHis(t)$$

$$\frac{dAcHis(t)}{dt} = k_2 Asa(t)\,His(t) - k_3 AcHis(t)$$

$$\frac{dAce(t)}{dt} = k_1 Asa(t) + k_3 AcHis(t)$$

Solution of these coupled, non-linear differential equations subject to the initial conditions: Asa(0) = Asa0, His(0) = His0, AcHis(0) = 0, and Ace(0) = 0 was obtained numerically using the DSolve command of the program Mathematica. Fits of the data shown in panels A and B of Fig. 1 indicate that the imidazole moiety of *N*α-acetylhistidine was acetylated rapidly, but that it rapidly broke down to yield the *N*α-acetylhistidine plus acetate. Under the conditions of these studies, we did not observe significant formation of the diamide derivative previously reported [28] to be formed from *N*τ,*N*π-diacetylhistidine, perhaps due to the minimal formation of the latter compound. Based on the analysis of the data in Fig. 1, values of the rate constants were $k_1 = 1.6 \times 10^{-2}$ hr^{-1}, $k_2 = 2.2 \times 10^{-4}$ mM^{-1} hr^{-1}, and $k_3 = 2.2 \times 10^{-1}$ hr^{-1} under the conditions of the study, $[\text{Aspirin}]_{t=0} = 37.8$ mM, $[\text{Histidine}]_{t=0} = 61.1$ mM, T = 37°, 212 mM phosphate (pH 7.0). The value of $k_1 = 1.6 \times 10^{-2}$ hr^{-1} = 0.384 day^{-1} was in reasonable agreement with the reported value of 0.343 day^{-1} determined in pH 7.4 buffer, at 30° [29]. For comparison, if we assume that the de-acetylation of aspirin is a base-catalyzed reaction, k_1 can be set equal to $k_1'[OH^-]$, giving $k_1' = 1.6 \times 10^5$ M^{-1} hr^{-1} at pH 7.0. Thus, the rate constant for reaction with hydroxide ion is ~ 7.2×10^5 times faster than the reaction of aspirin with the histidine imidazole nitrogen(s). This is an important result from the standpoint of protein acetylation, since it implies that histidine residues acetylated on the imidazole ring will be difficult to observe due to the transient nature of the species, and that acetylated histidine residues will tend to transfer acetyl groups to nearby residues.

The acetylation of 8.3 mM ubiquitin by 40 mM [1-^{13}C]acetylsalicylate over a period of 24 hr resulted in 6–8 resonances detected by long-range HMQC studies (Figs. 2A and 3). In these studies, the HMQC experiment was optimized for the two-bond $^2J_{CCH}$ coupling constant of 6.4 Hz between the acetyl methyl protons and C-1. For most of the studies reported here, we have utilized the acetyl methyl protons for detection, due to the greater sensitivity resulting from the presence of three equivalent protons. The effect of the amide protons was also apparent as an isotope shift of the acetyl C-1 resonance. Thus, it was possible to check that the resonances observed corresponded to amide linkages by working in a 50:50 H_2O:D_2O mixture. The resulting spectrum exhibited doubled C-1 resonances, with an apparent chemical shift difference

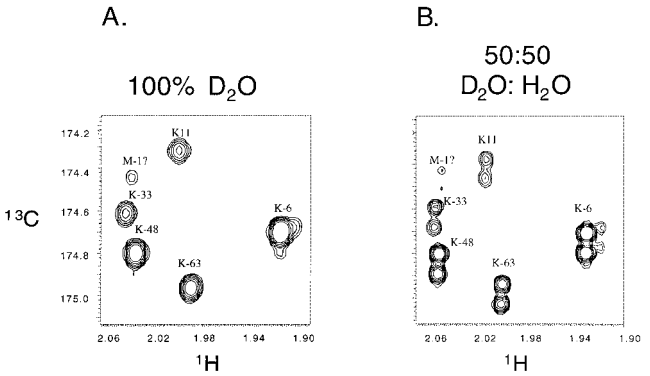

FIG. 2. (A) ^{1}H-^{13}C HMQC spectrum of acetylated ubiquitin obtained in 100% D_2O; (B) corresponding figure obtained in 50:50 D_2O:H_2O. Spectrum A corresponds to 8.3 mM acetylated ubiquitin at pH 7.0, while spectrum B was obtained at pH 7.4, so the resonance positions do not exactly correspond. Both samples are in 75 mM phosphate buffer, T = 37°.

$\Delta\delta(^{13}C) = 0.089$ ppm (Fig. 2B). Close inspection of Fig. 2B also reveals a very small δ isotope shift for the acetyl methyl protons of 0.0015 ppm. Formation of the amide linkage with the ϵ-amino group of lysine resulted in slowly exchanging amide protons, which also could be detected by the long-range HMQC experiment (Fig. 3). This spectrum was obtained at pH 4.82 in a 50:50 H_2O:D_2O mixture to sharpen the amide resonance by decreasing the effect of base-catalyzed exchange. Due to the pH difference of the acetylated ubiquitin NMR sample between the HMQC spectra displayed in Figs. 2 and 3, there was a noticeable chemical shift difference for two of the resonances (i.e. Lys-11 and Met-1). The ^{13}C shift of the downfield methyl resonance observed in the H_2O/D_2O solvent correlated with the proton amide resonance. A correlation to the ϵ-methylene proton resonances of lysine also could be detected. This study confirmed that the six major reso-

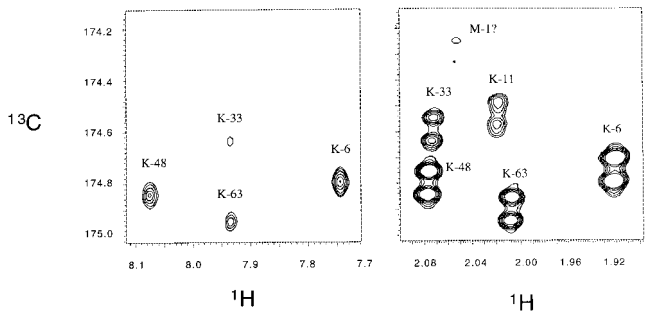

FIG. 3. ^{1}H-^{13}C HMQC spectrum of 8.3 mM acetylated ubiquitin at pH 4.82 obtained in 50:50 H_2O:D_2O, showing the correlation of the acetyl carbonyl ^{13}C shifts with the acetyl methyl proton shifts (right panel), and with amide proton shifts (left panel). The ^{13}C shifts in the left spectrum correspond to the downfield ^{13}C shifts of the methyl-correlated resonances. It is apparent that due to the lower sensitivity resulting from the presence of only one amide proton (vs three methyl protons) and from the 50:50 H_2O:D_2O mixture, only resonances corresponding to the more heavily acetylated residues are observed. The same sample as in Fig. 2 in 75 mM phosphate buffer, T= 37°.

nances seen with [1-^{13}C]acetylubiquitin corresponded to amide linkages formed with lysine and possibly with the N-terminal amino group, rather than to acetyltyrosine, acetylserine, acetylhistidine, or other possible derivatives.

A series of time-dependent acetylation studies indicated that there were significant differences in the rates of acetylation of the ubiquitin amino groups (Fig. 4). A linear fit of the first 4 data points gave an approximate initial rate of acetylation of the various adducts and permitted the determination of the relative reactivity (Fig. 4). The relative rates of residue acetylation for K6, K48, K63, K33, K11, and M1 thus were determined as 1.0, 0.59, 0.43, 0.26, 0.23, and 0.03, respectively. The apparent first order rate constant for acetylation of K6, neglecting time-dependent changes in aspirin concentration, was calculated as 0.25 M^{-1} hr^{-1}. Thus, differences in the reactivities of the various lysine residues with aspirin are quantitated readily. This differs from previous studies of ubiquitin acetylation, in which only approximate levels of acetylation by *p*-nitrophenylacetate could be established, and no information was obtained for several of the lysine residues.

To determine whether aggregation at the relatively high ubiquitin concentrations significantly influenced the relative reactivity, we treated solutions containing 0.5 and 2.1 mM wild-type ubiquitin with aspirin (see Materials and Methods). The relative intensities of the various adduct resonances were identical within the experimental error to the relative intensities derived from the 20-hr time point shown in Fig. 4.

Resonance Assignments

A variety of strategies are available for assignment of the acetyl resonances of the acetylated ubiquitin. The first approach considered is based on a correlation of the resonance intensities, and hence the degree of acetylation, with the fractional acetylation determined using an alternative methodology. For the acetylated ubiquitin, this was accomplished by comparing the degree of acetylation assessed from the NMR resonance intensities, with the fractional acetylation determined using an Edman degradation scheme, as outlined in Materials and Methods. A plot of the picomoles of lysine and acetyllysine based on the observation of PTH-ϵ-acetyllysine and PTH-ϵ-PTC lysine as a function of the Edman cycle is shown in Fig. 5. It is immediately apparent from the figure that, for example, Lys-6 was highly modified, while Lys-27 and Lys-29 were modified by less than a few percent. We note that although by the sixty-third cycle, the Lys-63 resonance yielded a fairly low intensity, expansion of the data in this region of the cycle indicated significant modification of this residue. The percentages of acetylation of the various residues, based on peak integration, are summarized in Table 2. One significant limitation of this approach is the potential failure to detect N-terminal acetylation of the protein, since this material will be resistant to the Edman degradation and will not contribute to the observed analysis. Hence, assignment of the resonances based on ranking of the degree of acetylation determined by the NMR and Edman methods could lead to a significant error. An independent method must therefore be used to evaluate N-terminal modification. Additionally, it is clear that for resonances that are acetylated to a similar degree, e.g. Lys-48 and Lys-63, no meaningful resonance assignment can be based on variations in the degree of acetylation.

A second assignment strategy makes use of available structural data on ubiquitin [14, 27]. For example, the sensitivity of resonance shifts to pH can to some extent be predicted by their location near titrable groups. The carbonyl ^{13}C shifts of [1-^{13}C]acetylubiquitin derived from the HMQC data were obtained as a function of pH (Fig. 6). Methyl proton shifts were also obtained in these studies, but proved to be less informative. Expectations based on the crystal structure are considered below. The proximity of acetyl-Lys-6 to His-48 located on the surface of the protein

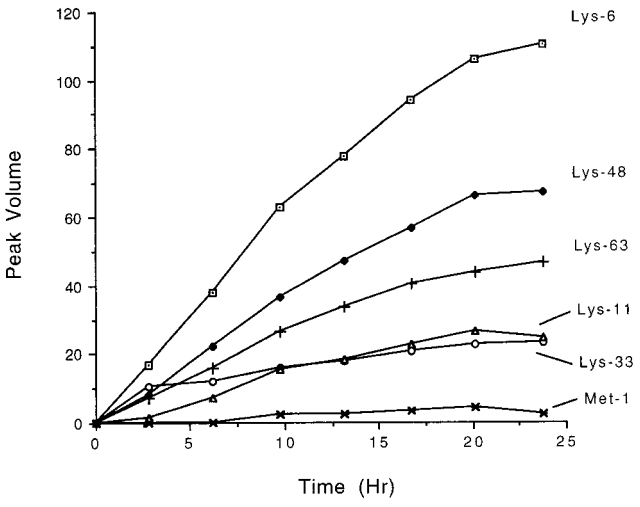

FIG. 4. Time-dependent resonance intensities of six acetylation sites. Note that the intensity scale here is arbitrary. Based on a comparison with an Edman degradation study performed on the same sample, the final percent acetylation of Lys-6 concentration is 18%.

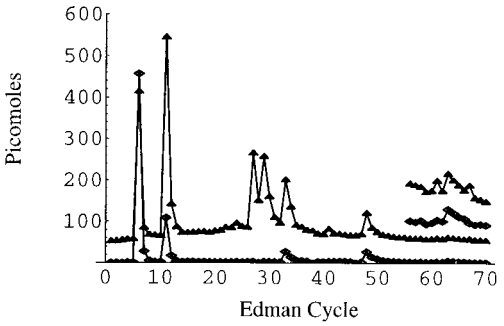

FIG. 5. Picomoles of lysine (▲) or Nϵ-acetyllysine (♦) derived from Edman degradation analysis. The inset shows an expansion of the data for cycles 56–70. This study utilized a higher [1′-^{13}C]acetylsalicylic acid concentration (120 mM), compared with the NMR study presented in Fig. 4.

TABLE 2. Solvent accessibility and percent modification of ubiquitin lysine residues

Residue	Solvent accessibility* 1.4 Å	Solvent accessibility* 3.0 Å	% Mod†	pK Values of dimethyl lysine residues‡	% Deprotonated§
Met-1	5.49	1.53	—	9.04	0.90
Lys-6	17.80	14.43	55.7	9.66	0.22
Lys-11	9.39	6.02	19.3	10.54	0.03
Lys-27	3.99	0.04	—	—	
Lys-29	11.15	6.81	—	10.12	0.08
Lys-33	13.30	8.29	23.5	10.02	0.10
Lys-48	12.12	9.03	40	9.76	0.17
Lys-63	16.23	10.36	38.7	10.12	0.08

*Contact areas determined using INSIGHT II and probe radii of 1.4 Å or 3.0 Å.
†Based on Edman degradation.
‡pK values of the dimethyl residues of reductively methylated ubiquitin, determined as described by LeBlanc *et al.* (manuscript in preparation).
§Percent of amino groups deprotonated at pH 7.0.

should result in a pH-dependent shift with pK in the range 6 to 7. 2. Both Lys-11 and Lys-27 are involved in salt bridge interactions with Glu-34 and Asp-52, respectively. The distances between the Lys ϵ-amino and the nearest carboxyl oxygen are 3.3 Å for Lys-11–Glu-34 and 2.9 Å for Lys-27–Asp-52. These interactions would be expected to depress the pK values for the Glu-34 and Asp-52 carboxyl groups. However, acetylation of the corresponding lysine residues will eliminate the salt bridge interaction, although hydrogen bonding interactions between the newly formed amide proton and the carboxyl oxygens are still possible. The proximity of the acetylated Lys-11 and 27 acetyl groups to these carboxyl groups should lead to significant pH-dependent shifts, with pK values typical of carboxyl side-chains. All of the above predictions are consistent with the assignments given in Table 2, made on the basis of the modification data. Thus, the acetyl carbonyl of Lys-6 exhibited a small but significant shift sensitivity with a pK of 5.7. Two resonances exhibited large, pH-dependent shifts with pK values of 4.8 and 4.4. Based on the data of Fig. 6, the resonance that exhibited a pK of 4.8 and that corresponded to the higher rate of modification could be assigned to Lys-11, in agreement with the initial assignment in Table 2. The less intense resonance could correspond to acetylated Lys-27, Lys-29, or to an acetylated Met-1 α-amino group. Of these possibilities, the N-terminal Met-1 amino group is the more plausible due to the presence of three relatively close carboxyl groups corresponding to Glu-16, Glu-18, and Asp-21. Additionally, it is possible that the observed pK arose from a conformational change that mediated the effect of titration of a remote carboxyl group. Interestingly, the resonances corresponding to these two acetyl carbonyl groups shifted in opposite directions with increasing pH (Fig. 6). This most probably indicated differences in the orientation of the acetyl C═O bond relative to the titrating carboxyl group, or possibly an indirect effect mediated by a conformational change, as suggested above. Unfortunately, the very low intensity of this resonance (Fig. 4) limits the use of various potential assignment strategies, so that the assignment of this resonance remains tentative.

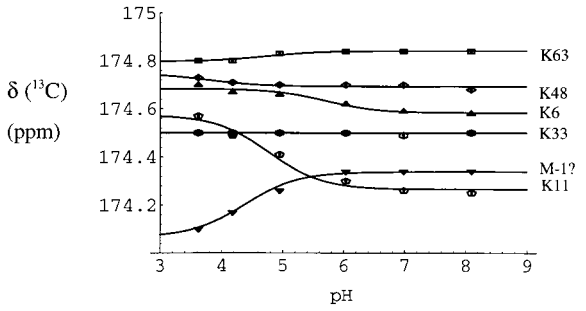

FIG. 6. Carbon-13 shifts of acetyl carbonyl group, derived from HMQC studies, as a function of pH for [1-^{13}C]acetylated ubiquitin. Resonances correspond to the acetyl groups on K6 (△), K11 (open pentagon), K33 (open hexagon), K48 (◇), K63 (□), and the unassigned acetyl group tentatively identified as the Met-1 terminal amino (▽).

To further confirm the assignments of the resonances that did not exhibit large pH-dependent shifts, we performed HMQC studies on two acetylated ubiquitin mutants: K33R and K63R (Fig. 7). The substitution of an arginine residue for a lysine is relatively conservative, preserving the charge, and is expected to introduce minimal structural perturbations, at least for lysines located on the surface of the protein. The resulting HMQC spectra provided unequivocal confirmation for the assignment of the acetylated Lys-33 and Lys-63 resonances.

Preparation and Study of Nitrated Ubiquitin

The presence of a single tyrosine residue in ubiquitin in close proximity to Lys-48 provides a potential basis for the further assignment of the acetyl-Lys-48 resonance. It has been demonstrated previously that this residue can be iodinated, with significant effect on activity in some assays [30] but not others [31, 32]. Nitration of the tyrosyl residues of proteins ortho to the hydroxyl group has been reported previously using tetranitromethane [24, 33–35]. Nitration lowers the pK of the tyrosyl hydroxyl group from 10.0 to 7.1 [33], and the resulting nitrotyrosine also exhibits cation

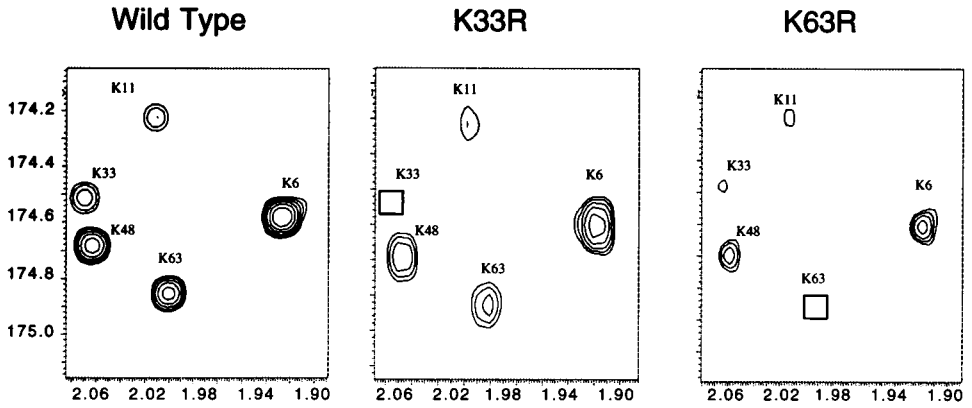

FIG. 7. HMQC spectra of acetylated ubiquitin (left panel); acetylated K33R (center panel); acetylated K63R (right panel). The missing resonance position is highlighted by the open square.

binding properties, which can make it useful for resonance assignment. Nitration of ubiquitin was performed as described in Materials and Methods, and the resulting nitrotyrosyl-59 ubiquitin was treated with [1′-^{13}C]aspirin analogously to the non-nitrated protein. HMQC studies of the acetylated nitrotyrosyl-59 ubiquitin gave ^{13}C data summarized in Fig. 8. In contrast with the data for non-nitrated ubiquitin (Fig. 6), the resonance assigned to Lys-48 showed a small (0.057 ppm) shift corresponding to a pK of 7.0, as determined from a non-linear fit to Eq. 1. The shifts of the remaining resonances were essentially identical to those of the non-nitrated, acetylated ubiquitin (Fig. 8). Hence, these data provide further support for the assignments of the acetyl resonances given in Table 2.

DISCUSSION

Aspirin has been found to acetylate many macromolecules *in vitro*, such as plasma proteins, enzymes, and DNA [36]. *In vivo* studies have revealed acetylation of a wide variety of proteins, glycoproteins, and lipids from various tissues [37] even though the serum half-life of aspirin is 20 min and only 68% of the dose reaches the systemic circulation [1]. Aspirin and sodium salicylates are prescribed in highest quantity for rheumatoid arthritis (3 g/day; 1–3 mM plasma concentration) [38], at concentrations where an additional mechanism of action occurs via inhibition of the transcription factor NF-κB [39]. To understand the biological and physiological effects of agents that modify proteins, it is necessary to understand the basic chemistry of their interactions with residues at the protein surface. Ubiquitin provides a relatively simple and stable model system for such studies. Total cellular ubiquitin concentration ranges from 80 to 100 μM, and therefore the ubiquitin-to-aspirin ratio of 1 to 15 used in this study is similar to that found with normal therapeutic doses of aspirin. The identification of acetylated serum albumin derived from the reaction with [2′-^{13}C]aspirin has been reported previously using 1D NMR techniques [23]. Although high selectivity of protein modification may be achieved in some cases, this is often not the case, and 2D NMR studies provide a useful and sensitive means for assessing the distribution of modified residues and ultimately for developing an understanding of the factors that influence residue reactivity. Two previous studies of the acetylation of ubiquitin by *p*-nitrophenyl acetate have been reported [19, 20]. In general, acetylation due to reaction with *p*-nitrophenyl acetate would be expected to exhibit a similar profile to modification by aspirin—both are aromatic compounds with similar size and molecular weight. However, this is not necessarily the case. For example, aspirin has been reported to acetylate serum albumin primarily at Lys-199 [4, 5], whereas *p*-nitrophenyl acetate has been reported to acetylate primarily Tyr-411 [40–42]. Although the earlier studies tended to be somewhat more qualitative, the results obtained here indicate a similar reaction profile for the two acetylating agents.

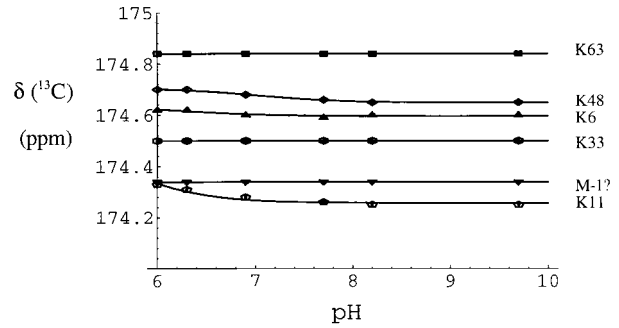

FIG. 8. Carbon-13 shifts of the acetyl carbonyl group, derived from HMQC studies, as a function of pH for [1-^{13}C]acetylated nitrotyrosyl ubiquitin. Resonances correspond to the acetyl groups on K6 (△), K11 (open pentagon), K33 (open hexagon), K48 (◇), K63 (□), and the unassigned acetyl group tentatively identified as the Met-1 terminal amino (▽).

In general, there is a fairly strong correlation between residue modification and surface accessibility, as determined based on the theoretical contact areas of the amino nitrogens using the Connolly algorithm. The most highly modified residue, Lys-6, is also the most accessible, while Met-1 Nα and Lys-27 Nε are relatively inaccessible and show very low degrees of modification. Since the aspirin molecule is considerably larger than the solvent water, the effects of increasing the probe size were also evaluated, and data corresponding to a probe radius of 3 Å are included in Table 2. The range of accessible contact areas becomes

TABLE 3. Lysine Nε distance matrix (Å)*†

	Lys-6	Lys-11	Lys-27	Lys-29	Lys-33	Lys-48	Lys-63
Lys-6		14	20	22	18	18	20
Lys-11	14		19	15	7	26	23
Lys-27	20	19		15	18	16	26
Lys-29	22	15	15		9	23	18
Lys-33	18	7	18	9		26	20
Lys-48	18	26	16	23	26		20
Lys-63	20	23	26	18	20	20	

*Based on crystal structure data of Vijay-Kumar *et al.* [27].
†Rounded to the nearest angstrom.

greater as the radius of the probe sphere is increased to 3 Å, so that the correlation of acetylation levels with accessibility becomes even stronger. The correlations with accessibility are not perfect, however, particularly for the low degree of modification of Lys-29, which contrasts with its relatively high solvent exposure. The ubiquitin crystal structure shows this residue curling back so that one of the amino protons hydrogen bonds to Glu-16 carbonyl oxygen. However, extension of the Lys-29 side chain to a more *trans* conformation leads to closer proximity to Asp-21, so that salt bridge interactions also could explain its low reactivity. Interestingly, in the diubiquitin [43] and tetraubiquitin [44] structures published, the distances between the Lys-29 Nε and the nearest carboxyl oxygen of Asp-21 are always shorter than the value published for the monomer; the shortest distances are 2.6 Å (tetraubiquitin) and 3.2 Å (diubiquitin) compared with 4.9 Å to the closest Asp-21 oxygen in the ubiquitin monomer.

We have determined recently the pK values for the dimethyl amino groups in reductively dimethylated ubiquitin*. As discussed by Vogel and coworkers [11, 12], these pK values are expected to approximate those of the free lysine or N-terminal amino residues. In general, the correlation of acetylation with these pK values is lower than with solvent accessibility (Table 2). Met-1, with the lowest pK value, is among the least modified amino groups. Lys-29 and Lys-63 have similar pK values but very different degrees of modification. The relatively high reactivity of Lys-6 is, however, consistent with the greater percentage of Nε in the unprotonated form.

Although the high reactivity of Lys-6 is consistent with its high solvent accessibility and low pK, the results obtained here with histidine suggest another possible basis for high levels of Lys-6 acetylation. Kinetic studies indicate that the imidazole ring of histidine is acetylated rapidly, but also rapidly transfers this acetyl group to water, yielding acetic acid. This result is not surprising, since acetylimidazole is itself an acetylating agent that has been used to acetylate proteins and other biomolecules [45]. The proximity of His-68 to Lys-6 suggests that it may play a role as an intermediate in the acetylation of Lys-6, such that acetyl groups are initially transferred to histidine and subsequently transferred from histidine to lysine. This suggests that, in general, lysine residues proximate to histidine side chains may be particularly susceptible to acetylation, and perhaps to other types of modification as well. Interestingly, it has been noted that the lysine residues of hemoglobin that are most readily acetylated by aspirin are near a histidine residue [7]. Hayden *et al.* [46] have found that the formation of difluorothionoacetyl-protein and lysine adducts from difluorothionoacetyl fluoride formed *in situ* can be catalyzed by the addition of *N*α-acetylhistidine or *N*α-acetyltyrosine. Nevertheless, the interpretation of such data is more complex, since the amino acids might act as catalysts but could also compete for the available acetyl groups, so that the effects will be dependent on the set of rate constants for the various transacetylation reactions.

Identification of the sixth HMQC resonance was hindered significantly by the very low degree of acetylation—only a few percent (Fig. 4). The most unique feature of this resonance was the sensitivity of the shift to one or more carboxyl titrations, which was in the opposite direction to that observed for the K11 acetyl group, which also shows significant pH sensitivity. Since the shift will in general depend on the orientation of the carbonyl group relative to the titrating carboxyl group, this result suggests a very different orientation for this group, relative to the K11 acetyl group. Based on proximity to other carboxyl groups, a preliminary assignment to acetylated Met-1 is most likely. This conclusion would differ significantly from previous reports indicating that *p*-nitrophenylacetate does not acetylate Met-1. However, as can be seen from Fig. 4, the degree of modification is very low.

One important aspect of NMR studies of protein modification is the potential of modified residues to interact with each other. The existence of such interactions is suggested by the Lys-6 resonance of Fig. 2, which shows small satellite peaks close to the primary HMQC resonance. These resonances could correspond to an additional acetylation site that exhibits a shift very similar to that of acetyl-Lys-6. An alternate explanation is that the modification of one or more of the other lysine residues, e.g. Lys-11, introduces a small but significant long-range perturbation of the shifts corresponding to acetyl-Lys-6, presumably mediated by a conformational perturbation. A

* LeBlanc DA, Haas AL and London RE, Manuscript in preparation.

distance matrix for the seven lysine ϵ-amino groups, derived from the crystal structure of Vijay-Kumar *et al.* [27] is shown in Table 3. As is apparent from this table, the terminal amino groups of the lysine residues of ubiquitin are fairly well separated, so that direct electrostatic effects on the shifts of one lysine due to acetylation of another would be minimal.

At a functional level, ubiquitin oligomers typically are involved in the ATP-dependent proteolysis reaction. Two crystal structures, corresponding to di- and tetraubiquitin, have been published [43, 44]. It is interesting to note that, from the standpoint of the environment of the lysine residues, the structure of the monomeric ubiquitin units in these structures differs rather markedly from the published structure of the monomer [27]. Thus, in the diubiquitin structure, the surface accessibility of K6 is much lower than the value in Table 2, and is in fact below the values for K27 and K29, which are also slightly lower than the values in Table 2. In the tetraubiquitin structure, the side chain amino group of one of the K6 residues appears to be hydrogen bonded to the G10 carbonyl oxygen (distance = 2.8 Å). Alternatively, a surface accessibility analysis indicates that the ϵ-amino group of K11 is the most accessible of all the ϵ-amino groups; the K11 Nϵ–E34 Oδ1 distance is now 6.2 Å, so there is no salt bridge. As is apparent from the data presented here, the results of the studies of acetylation of ubiquitin by aspirin are generally consistent with the accessibility of lysine residues predicted from the monomer structure, and clearly less compatible with accessibility and structural data for the monomers derived from the published dimer and tetramer structures. Since the dimer and tetramer structures were obtained at lower resolution (2.3 and 2.4 Å compared with 1.8 Å for the monomer), the differences in accessibility of the lysine residues may just reflect this fact. Alternatively, these results suggest significant conformational changes in the monomeric ubiquitin units upon oligomerization. These differences also highlight the general problem that the positions of surface lysine residues are typically determined with lower precision than most of the more structurally constrained residues. This behavior is particularly apparent in our recent studies of hemoglobin [47], which show large differences in orientation of the corresponding lysine residues between the two α or two β chains. Hence, the disorder of surface lysines tends to limit the usefulness of accessibility predictions based on crystallographic data.

The use of 2D HMQC NMR spectroscopy to obtain the time course of protein adduct formation by stable isotope labeled xenobiotics should prove widely useful in quantifying reactivity and determining specificity. This approach permits the rapid assessment of xenobiotic reactivity with relatively minimal labor. This is the first reported study utilizing 2D HMQC NMR spectroscopy to determine the relative rates of adduct formation of individual protein residues by a drug.

The authors are grateful to Dr. Olga Baboshina for development of the ubiquitin mutants, and to Joseph Vance and Eugene F. DeRose for technical assistance with the NMR studies. We thank Russell Henry for performing the protein sequencing and Carol Parker for technical support and consultation with mass spectroscopy during the initial stages of the assignment phase of this project. This work was supported in part by NIH Grant (GM 34009) to A. L. H.

References

1. Needs CJ and Brooks PM, Clinical pharmacokinetics of the salicylates. *Clin Pharmacokinet* **10:** 164–177, 1985.
2. Smith WL, Marnett LJ and DeWitt DL, Prostaglandin and thromboxane biosynthesis. *Pharmacol Ther* **49:** 153–179, 1991.
3. Marnett LJ, Aspirin and the potential role of prostaglandins in colon cancer. *Cancer Res* **52:** 5575–5589, 1992.
4. Walker JE, Lysine residue 199 of human serum albumin is modified by acetylsalicylic acid. *FEBS Lett* **66:** 173–175, 1975.
5. Hagag N, Birnbaum ER and Darnell DW, Resonance energy transfer between cysteine-34, tryptophan-214, and tyrosine-411 of human serum albumin. *Biochemistry* **22:** 2420–2427, 1983.
6. Klotz IM and Tam JWO, Acetylation of sickle cell hemoglobin by aspirin. *Proc Natl Acad Sci USA* **70:** 1313–1315, 1973.
7. Shamsuddin M, Mason RG, Ritchey JM, Honig GR and Klotz IM, Sites of acetylation of sickle cell hemoglobin by aspirin. *Proc Natl Acad Sci USA* **71:** 4693–4697, 1974.
8. Bridges KR, Schmidt GJ, Jensen M, Cerami A and Bunn HF, The acetylation of hemoglobin by aspirin *in vitro* and *in vivo*. *J Clin Invest* **56:** 201–207, 1975.
9. Bondoc LL and Timkovich R, Structural characterization of nitrimyoglobin. *J Biol Chem* **264:** 6134–6145, 1989.
10. Radford SE, Woolfson DN, Martin SR, Lowe G and Dobson CM, A three-disulphide derivative of hen lysozyme. Structure, dynamics and stability. *Biochem J* **273**, 211–217, 1991.
11. Zhang M and Vogel HJ, Determination of the side chain pK_a values of the lysine residues in calmodulin. *J Biol Chem* **268:** 22420–22428, 1993.
12. Zhang M, Thulin E and Vogel HJ, Reductive methylation and pK_a determination of the lysine side chains in Calbindin D_{9k}. *J Protein Chem* **13:** 527–535, 1994.
13. Zhang M, Huque E and Vogel HJ, Characterization of trimethyllysine 115 in calmodulin by ^{14}N and ^{13}C NMR. *J Biol Chem* **269:** 5099–5105, 1994.
14. Weber PL, Brown SC and Mueller L, Sequential ^{1}H NMR assignments and secondary structure identification of human ubiquitin. *Biochemistry* **26:** 7282–7290, 1987.
15. Wand AJ, Urbauer JL, McEvoy RP and Bieber RJ, Internal dynamics of human ubiquitin revealed by ^{13}C–relaxation studies of randomly labeled protein. *Biochemistry* **35:** 6116–6125, 1996.
16. Hochstrasser M, Protein degradation or regulation: Ub the judge. *Cell* **84:** 813–815, 1996.
17. Johnson PR and Hochstrasser M, SUMO-1: Ubiquitin gains weight. *Trends Cell Biol* **7:** 408–413, 1997.
18. Varshavsky A, The ubiquitin system. *Trends Biochem Sci* **22:** 383–387, 1997.
19. Jabusch JR and Deutsch HF, Localization of lysines acetylated in ubiquitin reacted with *p*-nitrophenyl acetate. *Arch Biochem Biophys* **238:** 170–177, 1985.
20. Zhu D-X, Xu L-X, Zhu N-Z, Briand G and Han K-K, *N*-epsilon-acetylation of porcine mature erythrocytes ubiquitin. *Int J Biochem* **17:** 719–721, 1985.
21. Hasan A, Smith JB, Qin W and Smith DL, The reaction of

bovine lens αA-crystallin with aspirin. *Exp Eye Res* **57:** 29–35, 1993.
22. Glocker MO, Borchers C, Fiedler W, Suckau D and Przybylski M, Molecular characterization of surface topology in protein tertiary structures by amino-acylation and mass spectroscopic peptide mapping. *Bioconjug Chem* **5:** 583–590, 1994.
23. Gerig JT, Katz KE, Reinheimer JD, Sullivan GR and Roberts JD, Examination of the aspirin acetylation site of human serum albumin by ^{13}C NMR spectroscopy. *Org Magn Reson* **15:** 158–161, 1981.
24. Riordan JF, Sokolovsky M and Vallee BL, Tetranitromethane: A reagent for the nitration of tyrosine and tyrosyl residues of proteins. *J Am Chem Soc* **88:** 4104–4105, 1966.
25. Ladner HK, Led JJ and Grant DM, Deuterium isotope effect on ^{13}C chemical shifts in amino acids and dipeptides. *J Magn Reson* **20:** 530–534, 1975.
26. Baboshina OV and Haas AL, Novel multiubiquitin chain linkages catalyzed by the conjugating enzymes $E2_{EPF}$ and RAD6 are recognized by 26 S proteasome subunit 5. *J Biol Chem* **271:** 2823–2831, 1996.
27. Vijay-Kumar S, Bugg CE and Cook WJ, Structure of ubiquitin refined at 1.8 Å resolution. *J Mol Biol* **194:** 531–544, 1987.
28. Welsch DJ and Nelsestuen GL, Irreversible degradation of histidine-96 of prothrombin fragment 1 during protein acetylation: Another unusually reactive site in the kringle. *Biochemistry* **27:** 7513–7519, 1988.
29. Kelly CA, Determination of the decomposition of aspirin. *J Pharm Sci* **59:** 1053–1079, 1970.
30. Pickart CM, Haldeman MT, Kasperek EM and Chen Z, Iodination of tyrosine 59 of ubiquitin selectively blocks ubiquitin's acceptor activity in diubiquitin synthesis catalyzed by $E2_{25K}$. *J Biol Chem* **267:** 14418–14423, 1992.
31. Haas AL and Rose IA, The mechanism of ubiquitin activating enzyme. A kinetic and equilibrium analysis. *J Biol Chem* **257:** 10329–10337, 1982.
32. Haas AL, Warms JV, Hershko A, and Rose IA, Ubiquitin-activating enzyme: Mechanism and role in protein-ubiquitin conjugation. *J Biol Chem* **257:** 2543–2548, 1982.
33. Snyder GH, Rowan R III, Karplus S and Sykes BD, Complete tyrosine assignments in the high field ^{1}H nuclear magnetic resonance spectrum of the bovine pancreatic trypsin inhibitor. *Biochemistry* **14:** 3765–3777, 1975.
34. Marinetti TD, Snyder GH and Sykes BD, Nitrotyrosine chelation of nuclear magnetic resonance shift probes in proteins: Application to bovine pancreatic trypsin inhibitor. *Biochemistry* **16:** 647–653, 1977.
35. Skawinski WJ, Adebodun F, Cheng JT, Jordan F and Mendelsohn R, Labeling of tyrosines in properties with [^{15}N]tetranitromethane, a new NMR reporter for nitrotyrosines. *Biochim Biophys Acta* **1162:** 297–308, 1993.
36. Pinckard RN, Hawkins D and Farr RS, *In vitro* acetylation of plasma proteins, enzymes and DNA by aspirin. *Nature* **219:** 68–69, 1968.
37. Rainsford KD, Schweitzer A, and Brune K, Distribution of the acetyl compared with the salicyl moiety of acetylsalicylic acid: Acetylation of macromolecules in organs wherein effects are manifest. *Biochem Pharmacol* **32:** 1301–1308, 1983.
38. Rainsford KD, *Aspirin and Salicylates*. Butterworths, London, 1984.
39. Kopp E and Ghosh S, Inhibition of NF-κB by sodium salicylate and aspirin. *Science* **265:** 956–959, 1994.
40. Sollenne NP and Means GE, Characterization of a specific drug binding site of human serum albumin. *Mol Pharmacol* **14:** 754–757, 1979.
41. Ozeki Y, Kurono Y, Yotsuyanagi T and Ikeda K, Effects of drug binding on the esterase activity of human serum albumin: Inhibition modes and binding sites of anionic drugs. *Chem Pharm Bull* **28:** 535–540, 1980.
42. Kurono Y, Ozeki Y, Yamada H, Takeuchi T and Ikeda K, Effects of drug bindings on the esterase-like activity of human serum albumin. VII. Subdivision of R-type drugs inhibiting the activity towards *p*-nitrophenyl acetate. *Chem Pharm Bull* **35:** 734–739, 1987.
43. Cook WJ, Jeffrey LC, Carson M, Chen Z and Pickart CM, Structure of a diubiquitin conjugate and a model for interaction with ubiquitin conjugating enzyme (E2). *J Biol Chem* **267:** 16467–16471, 1992.
44. Cook WJ, Jeffrey LC, Kasperek E and Pickart CM, Structure of tetraubiquitin shows how multiubiquitin chains can be formed. *J Mol Biol* **236:** 601–609, 1994.
45. Wells I and Marnett LJ, Acetylation of prostaglandin endoperoxide synthetase by *N*-acetylimidazole: Comparison to acetylation by aspirin. *Biochemistry* **31:** 9520–9525**,** 1992.
46. Hayden PJ, Yang Y, Ward AJI, Dulik DM, McCann DJ and Stevens JL, Formation of difluorothionoacetyl-protein adducts by *S*-(1,1,2,2-tetraflouroethyl)-L-cysteine metabolites: Nucleophilic catalysis of stable lysyl adduct formation by histidine and tyrosine. *Biochemistry* **30:** 5935–5943, 1991.
47. Xu ASL, MacDonald JM, Labotka RJ and London RE, NMR study of the sites of human hemoglobin aceylated by aspirin. *Biochem Biophys Acta*, in press.